

See discussions, stats, and author profiles for this publication at: <https://www.researchgate.net/publication/324007368>

# Xsens MVN: Consistent Tracking of Human Motion Using Inertial Sensing

Technical Report · March 2018

DOI: 10.13140/RG.2.2.22099.07205

---

CITATIONS

67

READS

18,510

3 authors, including:



Martin Schepers

Xsens

48 PUBLICATIONS 1,282 CITATIONS

[SEE PROFILE](#)



Matteo Giuberti

Xsens

20 PUBLICATIONS 389 CITATIONS

[SEE PROFILE](#)

Some of the authors of this publication are also working on these related projects:



Vrehab [View project](#)



MiniSens [View project](#)

# Xsens MVN: Consistent Tracking of Human Motion Using Inertial Sensing

Martin Schepers, Matteo Giuberti, and Giovanni Bellusci

**Abstract**—Xsens MVN is an easy to use, cost efficient system that captures full-body human motion in any environment. It is based on small, unobtrusive inertial and magnetic sensors combined with advanced algorithms and biomechanical models. The newly released motion capture engine is immune to magnetic distortions and is available either as MVN Animate for the 3D character animation market, or as MVN Analyze for the human motion measurement market. This whitepaper describes key characteristics and shows an analysis of the performance of the new engine. The performance analysis includes a comparison with an optical position measurement system in combination with OpenSim for walking data, as well as a consistency analysis for running data. The analysis shows RMS differences of less than 5 degrees for the dominant joint angles during walking and consistent performance over more than 90 minutes of running data. The MVN Analyze and MVN Animate engines enable reliable and consistent tracking of any type of movement including running, jumping, squatting, crawling, cartwheeling, in any type of environment, including severe magnetically distorted environments.

## I. INTRODUCTION

OVER the past decade, inertial motion capture has been used by a growing community and in a wide range of applications varying from character animation for movies, games, augmented reality and virtual reality, as well as human motion measurements for biomechanics, rehabilitation, ergonomics and sports.

Compared to alternative motion capture systems based on external emitters and/or cameras, inertial motion capture does not rely on any external infrastructure allowing it to be used anywhere [1]. Despite this huge advantage over alternative motion capture systems, inherent drift of orientation (and position) in current solutions has prevented inertial motion capture systems to become a commodity. Segment positions and orientations are typically estimated by applying the result of a sensor-to-segment calibration procedure to the corresponding sensor orientation estimates, and applying it to a (scaled) biomechanical model of the human body [2]. Each of these three components introduces errors that may affect performance, which will be individually discussed in the remainder of this paragraph. First, sensor-to-segment calibration is typically obtained by asking the subject to stand in a known pose (e.g. N-pose or T-pose) and estimating the sensor orientations by combining the sensor readings of the accelerometer (inclination) and magnetometer (heading), much like using a water level and a compass needle. Specifically the direct use



Fig. 1. Xsens MVN consists of 17 inertial and magnetic motion trackers. Data from wireless (*MVN Awinda*) or wired (*MVN Link*) trackers is transmitted by a wireless connection to a PC where the data is further processed and visualized.

of the magnetometer readings to obtain heading is a major source of error, since magnetic distortions or magnetometer calibration errors significantly affect the overall accuracy [3]. Furthermore, the assumption of the subject holding a predetermined pose is likely to be (at least partly) violated, thus possibly leading to orientation errors that exceed 5 degrees [4]. Second, individual sensor orientation is typically obtained by fusing the signals from the accelerometer, gyroscope, and magnetometer in a sensor fusion framework (e.g. complementary or Kalman filtering [5]–[7]). Short-term changes in orientation are accurately tracked by the gyroscope, while the accelerometer and magnetometer provide longer-term stability. Accuracy depends on both sensor calibration and environment conditions. Inclination estimates can be distorted by long-term accelerations, while heading estimates can be corrupted by magnetic distortions, for instance from common materials in buildings (steel constructions, reinforced concrete, etc.), furniture, and electronic equipment in the surroundings. Despite the huge improvements in accuracy of single sensor orientation tracking, there are fundamental limits to the accuracy that can be obtained using gyroscopes, accelerometers, and magnetometers alone. Third, the biomechanical model has limited accuracy when applied to a wide range of subjects. Imperfections in scaling of the model and inaccurate estimates

of sensor locations on the segments are examples of error sources affecting the overall accuracy.

In the past years, Xsens has spent tremendous efforts towards the creation of a new motion capture engine that aims at overcoming the major error sources of current solutions, in order to provide an accurate and consistent solution. The new engine combines the data of all motion trackers with advanced biomechanical models resulting in an immunity to the effects of magnetic distortions. In addition, the sensor-to-segment calibration procedure no longer relies on the data from the magnetometers, allowing the calibration to be performed anywhere. Finally, although the assumption of a known pose (N/T-pose) together with a predefined scaling model is still used in the current version of the engine, the current framework allows inclusion of customized models.

This paper describes the architecture of the Xsens MVN system together with some key features of the accompanying software. The performance of the newly released engine is shown by a comparison with an optical reference system to demonstrate its accuracy and consistency.

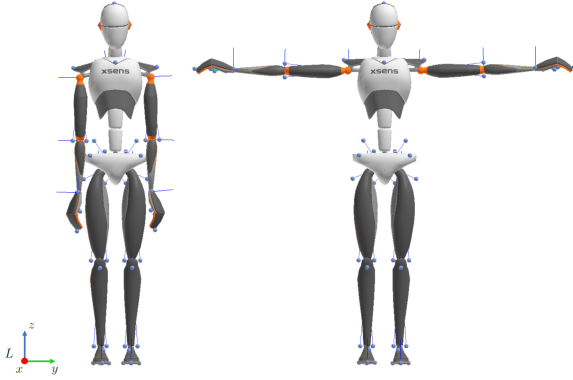


Fig. 2. Xsens MVN avatar in N-pose (left) and T-pose (right). In the T-pose, all segment coordinate frames are aligned with the common coordinate frame  $L$  shown at the bottom left.

## II. XSENS MVN ARCHITECTURE

Xsens MVN is a motion capture system consisting of hardware and software, each available in specific versions to accommodate customer and market needs. This section gives an overview of both the hardware and software of Xsens MVN.

### A. Xsens MVN Hardware

The hardware of Xsens MVN (Fig. 1) is available as a body-wired solution that streams data wirelessly to a PC/laptop (*MVN Link*) and a completely wireless solution (*MVN Awinda*). To capture the motion of the human body, 17 motion trackers are attached to the feet, lower legs, upper legs, pelvis, shoulders, sternum, head, upper arms, fore arms, and hands. The sensor modules are inertial and magnetic measurement units that contain 3D gyroscopes, 3D accelerometers and 3D magnetometers. Each module runs an advanced signal processing pipeline that includes patented StrapDown Integration (SDI) [8]–[15] algorithms to send the

data at a relatively low rate (e.g. 60Hz), while preserving the accuracy of sampling at a much higher rate (e.g. >1kHz). Due to the use of SDI, 3D tracking accuracy of each motion tracker is equivalent both for *MVN Link* (240Hz) as well as *MVN Awinda* (60Hz), with only a reduced time resolution for the latter. Hence, for high dynamic movements including frequent interactions with the floor (contacts), *MVN Link* is recommended.

1) *MVN Link*: *MVN Link* consists of wired motion trackers (MTx) that are connected to an on-body data hub (BodyPack) responsible for gathering data and providing power. A custom lycra suit takes advantage of dedicated zippers for a simplified mounting of motion trackers at specific body locations. The combined data of all motion trackers is wirelessly transmitted by the BodyPack over Wifi to a PC/laptop/tablet using the (soft) access point. An additional feature of *MVN Link* is to use On-Body Recording (OBR) which allows movements to be recorded without the need of the PC/laptop/tablet by storing the data on internal memory of the BodyPack for up to 15 hours. The dimensions of an MTx are 36 x 24.5 x 10 mm, with a total weight of 10 g. The BodyPack dimensions are 160 x 72.5 x 25 mm, and it weighs 150 g. The dimensions of the associated battery pack are 94.7 x 58.5 x 25 mm, and its weight is 70 g. The total battery life of the system during normal use is 10 hours.

2) *MVN Awinda*: *MVN Awinda* is similar to *MVN Link*, but instead uses wireless motion trackers (MTw) and body straps. Data is transmitted wirelessly between each motion tracker and the so-called Awinda Station using a patented protocol [8]–[11]. Each MTw (size 47 mm, 30 mm x 13 mm, weight 20 g) has the same sensing components as an MTx, but additionally includes a battery and a transceiver. The battery life of *MVN Awinda* is 6 hours.

### B. Xsens MVN Software

The key element of Xsens MVN is the software engine, where the SDI data of the individual motion trackers is combined with biomechanical models of the human body to obtain segment positions and orientations. The customers and applications of Xsens MVN can be roughly categorized in two main market segments, each characterized by specific needs: the 3D Character Animation (3DCA) market, including games and movies; and the Human Motion Measurement (HMM) market, which includes ergonomics, sports, and research. Since the applications and needs of each market can be rather different, Xsens offers a customized engine for each of the two markets: MVN Animate for the 3DCA market, and MVN Analyze for the HMM market.

Both engines offer two processing modes. For *realtime* and (*automatic*) *reprocessing*, the data is processed frame by frame, progressing forward in time. The engine combines the data of all motion trackers with advanced biomechanical models to obtain the position and orientation of all human body segments. The *reprocess HD* mode adds the feature of processing data over a larger time window to get an optimal (and more consistent) estimate of the position and orientation of each body segment.

Within the software, four user scenarios are available which mainly differ in the handling of interactions with the environment (floor interactions):

- *Single Level*: This is the default scenario that should be used when interactions of the subject are known to be limited to a single level. The behavior of the contact points, which can be anywhere on the body, is confined to a zero level floor. If the subject is for example climbing some stairs, each step is corrected towards the zero level floor and the height information is lost.
- *Multi Level*: The use of the *Multi Level* scenario is recommended for subjects who interact with floors/objects that are not strictly single level, e.g. during stair climbing, sitting, etc. However, it should be noted that some minor drift in height may still occur.
- *No Level*: For users who are not primarily interested in floor interaction and position changes with respect to the environment, the *No Level* scenario is recommended, since in this scenario the pelvis is fixed in space and all kinematic quantities are expressed relative to the pelvis. This scenario is especially suited for the analysis of human body joint angles in biomechanics, or for applications in which ground contacts are not clearly defined, e.g. ice skating.
- *Soft Floor*: This scenario is intended for cases where floor interaction with a single level floor is important, but the floor is not strictly a zero level, such as when walking on a soft surface.

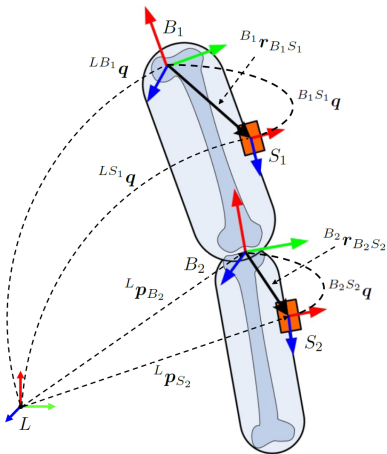


Fig. 3. Schematic overview of two connected segments ( $B_1$  and  $B_2$ ) with corresponding sensors ( $S_1$  and  $S_2$ ), and relevant coordinate frames and variables.

### III. MOTION TRACKING

Xsens MVN tracks the motion of the human body [16]–[21] defined with a biomechanical model consisting of 23 segments, being the pelvis, L5°, L3°, T12°, T8, neck°, head, shoulders, upper arms, lower arms, hands, upper legs, lower legs, feet and toes°. The segments indicated with a ° do not have a sensor attached and their movement is estimated by combining

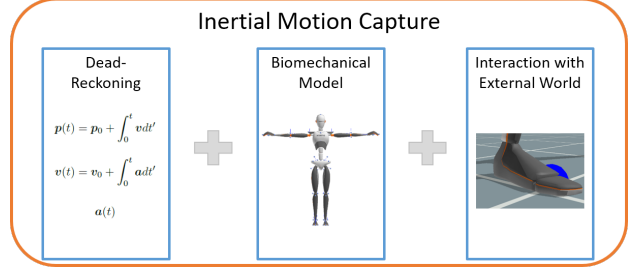


Fig. 4. Schematic overview of the main components required to perform inertial motion capture.

the information of connected segments and the biomechanical model.

For each body segment  $B$ , all kinematic quantities are expressed in a common, local coordinate frame  $L$ , which is a right-handed Cartesian coordinate system defined by:

- $X$  positive when moving forward, and lying in the horizontal plane. This axis is defined by the user during subject calibration (Sec. III-A).
- $Y$  pointing lateral, and orthogonal to  $X$  and  $Z$  according to the right-handed coordinate system.
- $Z$  along the vertical, gravity referenced, positive when pointing up.

The coordinate axes of each segment  $B$  are defined such that they are aligned with the coordinate frame  $L$  when the subject is standing in the T-pose as shown in Fig. 2.

Fig. 3 shows an overview of two connected segments ( $B_1$  and  $B_2$ ), with two sensors ( $S_1$  and  $S_2$ ) attached to them, and the associated relations for position and orientation. Typical human body motion tracking systems obtain the position of each segment ( ${}^L\mathbf{p}_{B_1}$  and  ${}^L\mathbf{p}_{B_2}$ ), and orientation ( ${}^{LB_1}\mathbf{q}$  and  ${}^{LB_2}\mathbf{q}$ , expressed as a quaternion [22]) of each segment with respect to the local frame  $L$ , by applying advanced sensor fusion algorithms to the measured acceleration, angular velocity, and magnetic field as indicated by Fig. 4. These sensor fusion algorithms aim at exploiting specific features of the available signals, which in case of inertial and magnetic sensors are complementary to each other. The relation between the position and orientation of each segment ( ${}^L\mathbf{p}_B$  and  ${}^L\mathbf{q}$ ) and corresponding sensor ( ${}^L\mathbf{p}_S$  and  ${}^L\mathbf{q}$ ) is typically obtained by applying the results of a sensor-to-segment calibration procedure (Sec. III-A2) to the orientation:

$${}^{LB}\mathbf{q} = {}^{LS}\mathbf{q} \otimes {}^{BS}\mathbf{q}^*, \quad (1)$$

and the position

$${}^L\mathbf{p}_B = {}^L\mathbf{p}_S + {}^{LB}\mathbf{q} \otimes {}^B\mathbf{r}_{BS} \otimes {}^{LB}\mathbf{q}^*, \quad (2)$$

where  ${}^{BS}\mathbf{q}$  denotes the relative orientation of the sensor with respect to the body,  ${}^B\mathbf{r}_{BS}$  denotes the position of the sensor with respect to the segment origin expressed in the segment frame,  $\otimes$  denotes the quaternion multiplication and  ${}^*$  denotes the complex conjugate of the quaternion [22]. Note that the subscripts,  $_1$  and  $_2$ , to indicate the segment and sensor in Fig. 3 have been omitted for clarity.

Starting with the sensor orientation, the integration over time of the angular velocity measured by the gyroscope gives

a high-bandwidth and responsive estimate of the change in orientation, but it is prone to integration drift. The addition of the gravitational and magnetic components, obtained from the accelerometer and magnetometer respectively, gives stabilizing information on the long term. The resulting absolute orientation is accurate, but fundamentally limited by the accuracy of the stabilizing information (i.e. acceleration for inclination and, especially, magnetic field for heading). For the tracking of single sensor orientation, Xsens has more than 15 years of experience in applying advanced modeling and practical application knowledge to provide a consistent orientation estimate that matches the application [23], [24]. This becomes especially important in difficult situations closer to these fundamental limits.

To get an estimate of the change in position, the sensor's free acceleration (i.e. compensated for gravity by applying the estimated sensor orientation and removing the gravitational acceleration) is double integrated. The resulting (relative) position provides an accurate prediction for short periods of time, but over time will inherently drift due to orientation estimation errors as well as sensor errors. By applying biomechanical models in combination with advanced contact detection algorithms, an accurate and drift-free estimate of the relative position and orientation of the individual body segments is obtained, as well as the position of the body with respect to the environment. An additional aspect to take into account is the connection between a sensor and a segment, which is not a rigid connection, but instead may fluctuate significantly depending on the amount of soft tissue (e.g. skin, clothes, etc.) between them. If not accounted for, this may result in inaccurate tracking of the body segments [25].

The newly available engine includes advanced models and intelligent, carefully formulated assumptions such that the resulting motion being tracked is consistent and immune to magnetic distortions, especially when processed using the *reprocess HD* mode. The engine is flexible and allows to integrate other sources of information, for example position aiding using optical/RF/GNSS/UWB/etc. [26]–[29], or force/pressure sensing [30], to improve and enrich the overall estimation.

Some additional aspects related to the subject calibration and the extraction of the joint angles are discussed in the remainder of this section.

#### A. Subject calibration

The purpose of subject calibration is to estimate the dimensions/proportions of the person being tracked, as well as the orientation of the sensors with respect to the corresponding segments.

1) *Scaling*: The dimensions are obtained by applying a generalized scaling model to a set of input parameters given by the user. As a minimum, this consists of the body height and foot length, but can be extended with additional measurements including arm span, ankle height, hip height, hip width, knee height, shoulder width, shoulder height, and extra sole height. Based on the generalized model, the engine finds the best fit from the given parameters.

2) *Sensor-to-Segment Calibration*: To be able to estimate the segment kinematics using measurements from the sensors, the alignment between sensors and segments needs to be known. Since no explicit measure of segment poses is directly available, a reference pose is used where segment orientations are assumed to be known. In Xsens MVN, this is done in a dedicated calibration procedure where the subject is asked to stand still in N-pose (recommended) or T-pose (see Fig. 2), and to walk a few meters back and forth for a short period of time. Note that, while assuming the static pose, the quality of the performed pose is crucial, since the segment orientations are assumed to be known. The major advantage over the formerly used static pose is that this method is immune to the effects of magnetic distortions, making its use possible and effective in any environment.

3) *Axes definition*: After completion of the sensor-to-segment calibration procedure, the subject is asked to apply the calibration while standing in N/T-pose facing the forward direction of the measurement environment. In this way, the forward *X* direction of the local *L* coordinate system is defined as well as its origin (which is defined at the position of the right heel). In case of multiple subjects in a session, this procedure is necessary to define a common reference system for all subjects. During the session, the user can still reset the heading direction as well as the position of the subject.

#### B. Joint angles

In many biomechanical applications, the user might be interested in knowing the joint angles rather than the individual segment kinematics. In Xsens MVN, we therefore provide these joint angles directly using joint definitions based on the ISB recommendations for standardization in the reporting of kinematic data [31]–[33]. To follow these recommendations, Xsens MVN uses an intermediate frame for calculation purposes only. This frame is defined for each segment to closely match the ISB recommendations, but differs from the general Xsens MVN coordinate frame earlier described in this section in that it has the *Y*-axis aligned with the vertical, *X* pointing forward, and *Z* pointing lateral. The coordinate axes of each segment are aligned with this intermediate frame when the subject is standing in the anatomical pose, which is close to the N-pose, but differs in terms of the palms of the hands which in this case are facing forward.

The joint angles are extracted by first calculating the difference between the orientation of the distal segment  ${}^{LB_1}\mathbf{q}$  and the proximal segment  ${}^{LB_2}\mathbf{q}$  (Fig. 3):

$${}^{B_1 B_2} \mathbf{q} = {}^{LB_1} \mathbf{q}^* \otimes {}^{LB_2} \mathbf{q}. \quad (3)$$

Subsequently, this quaternion is converted to Euler angles following the ISB and Grood and Suntay recommendations [34]. All Xsens MVN joint angles follow the extraction order of *Z* for flexion/extension, *X* for abduction/adduction and *Y* for internal/external rotation. For the shoulders, also the XZY sequence is available. It should be noted that the names of some angles might be different for some joints, i.e. dorsiflexion/plantarflexion for the ankles, pronation/supination for the elbows and wrists, and lateral bending and axial rotation for the spine, neck, and head segments.

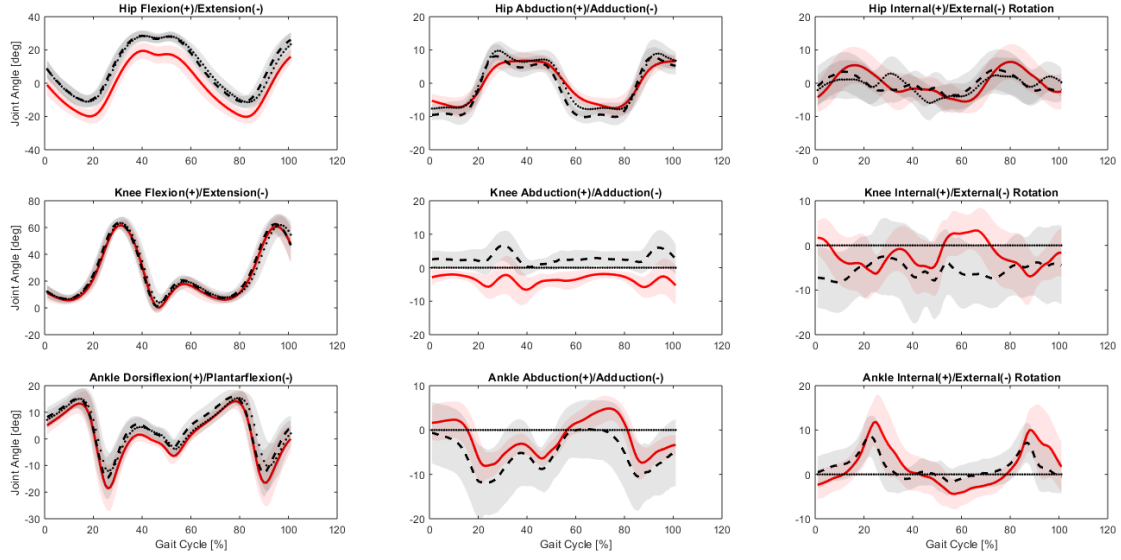


Fig. 5. Comparison of the joint angles of both legs for hip, knee, and ankle for walking at normal speed using three processing modes: MVN Analyze (red solid); OpenSim RDOF (black dots); and OpenSim FDOF (black dashed). Gait cycles are time-normalized and averaged over all subjects. Standard deviations of each angle are indicated by the semi-transparent areas.

TABLE I

TABLE SHOWING THE RMS DIFFERENCES (MEAN (STANDARD DEVIATION)) BETWEEN MVN ANALYZE AND OPENSIM FDOF DURING WALKING. EACH COLUMN INDICATES THE JOINT ANGLE (FLEXION/EXTENSION (FE), ABDUCTION/ADDITION (AA), INTERNAL/EXTERNAL ROTATION (IE)) OF THE HIP, KNEE AND ANKLE (ROWS).

	FE [deg]	AA [deg]	IE [deg]
Hip	10.1 (5.6)	3.8 (1.2)	6.2 (4.2)
Knee	3.2 (1.5)	7.3 (2.9)	7.4 (3.4)
Ankle	4.5 (1.8)	6.9 (2.2)	5.8 (1.6)

TABLE II

TABLE SHOWING THE RMS DIFFERENCES SIMILAR TO TABLE I, BUT WITH THE STATIC POSE FROM THE OPTICAL DATA FOR CALIBRATION.

	FE [deg]	AA [deg]	IE [deg]
Hip	4.8 (2.9)	3.7 (1.8)	5.7 (2.9)
Knee	3.7 (2.2)	4.4 (1.7)	8.0 (3.4)
Ankle	4.7 (2.3)	7.2 (2.6)	5.7 (2.2)

#### IV. PERFORMANCE ANALYSIS

MVN Analyze is the recommended engine for biomechanical analysis. In particular, for analysis of joint angles, the *No Level* scenario in the *reprocess HD* mode is the suggested engine configuration. Two different sets of data, i.e. walking and running, have been used to demonstrate accuracy and consistency of this new engine.

##### A. Walking

The first dataset consisted of a group of 8 healthy young participants (2 females and 6 males) who were asked to walk back and forth in a laboratory environment at three different speeds (slow, normal, and fast). Data was captured using MVN Link and, at the same time, optical data was

captured for comparison using an 8-camera Qualisys system. The objective of this dataset was to show the accuracy of joint angles estimated using MVN Analyze, by comparing them with those obtained by processing the optical data with OpenSim [35]. Hip, knee, and ankle angles (flexion/extension (FE), abduction/adduction (AA), and internal/external rotation (IE)) are estimated for each trial in MVN Analyze using the *No Level* scenario in the *reprocess HD* mode. The optical data is processed using OpenSim [35] with two processing options, being the standard Gait 2392 model, which constrains the knee and ankle to a single degree of freedom with a separate subtalar joint (OpenSim RDOF), and a modified version which models the knee and ankle as a 3D joint (OpenSim FDOF). Both models apply an inverse kinematics solver to the optical data from which the joint angles are extracted.

Fig. 5 shows a comparison between MVN Analyze and OpenSim (FDOF and RDOF) where columns indicate the three different joint angles and rows represent the hip, knee, and ankle. The figure shows overall good correspondence between MVN Analyze and OpenSim joint angles, which is also reflected by the RMS differences reported in Table I. The dominant angle during walking is the flexion/extension angle, which shows excellent correspondence especially for the knee and ankle angles. Although the joint angle profiles are generally matching, it is sometimes possible to notice some offsets between MVN Analyze and OpenSim estimates, especially for hip flexion/extension and knee abduction/adduction. This similarity in shape together with the presence of offsets is also observed in literature [36], and is likely to be attributed to the combination of subject calibration in Xsens MVN, and marker placement of the optical system. In Xsens MVN we need to assume a known pose during calibration (Sec. III-A2), in which the person is asked to stand in the N-pose or T-

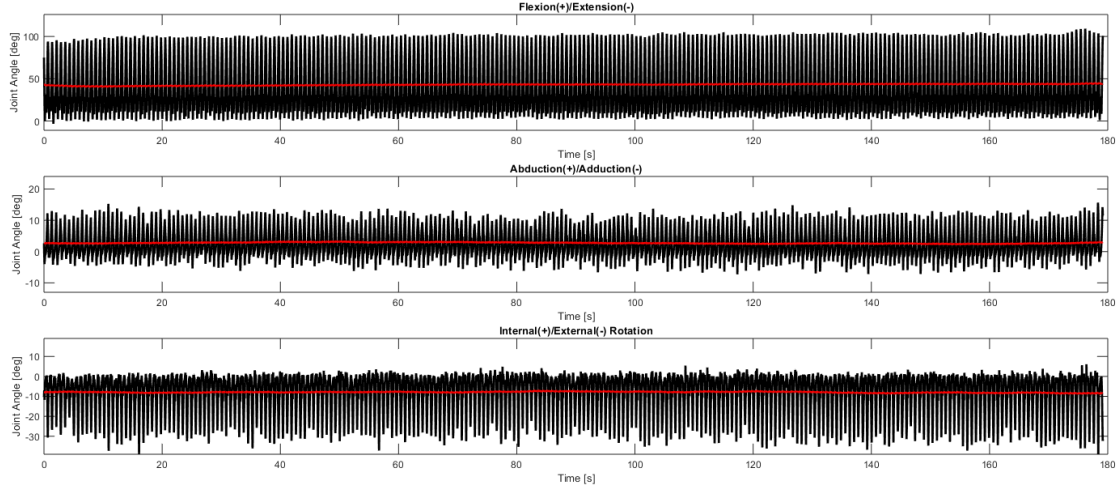


Fig. 6. Right knee joint angles in black (flexion/extension, abduction/adduction, and internal/external rotation) during running on a treadmill. The red line shows the average joint angle by applying a moving average over 10s.

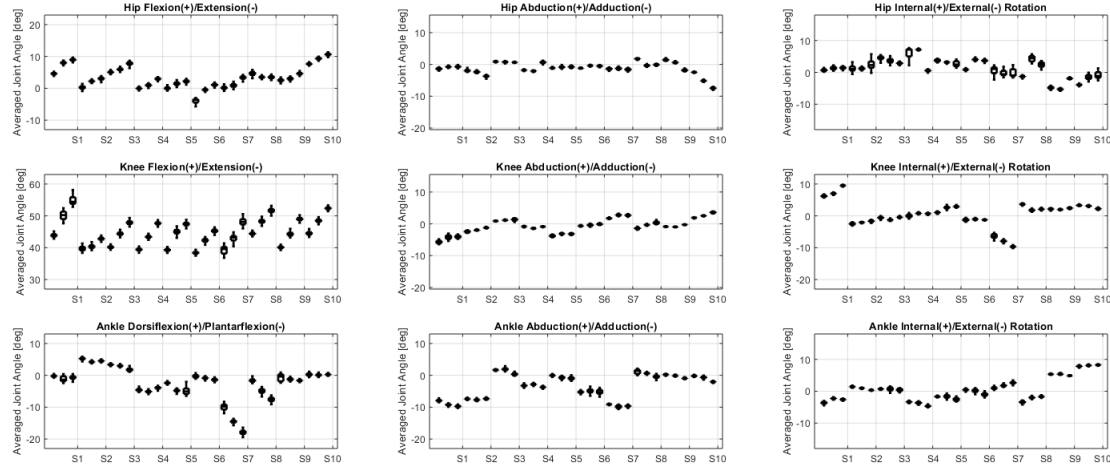


Fig. 7. Box and whisker plot of all averaged joint angles of the right leg for hip, knee and ankle during all 30 running trials. The trials are ordered by the 3 different speeds (10, 12, and 14 km/h) for each subject (S1 - S10), visually separated by the vertical lines. The box edges indicate the 25th and 75th percentiles, and the line indicates the median. The whiskers extend to the most extreme data points not considered outliers.

pose. During this static pose, body segments are assumed to be aligned with the reference pose, whereas the static pose from the optical is directly measured using the positions of the markers attached to the bony landmarks. Several studies indicate offsets and variability of segments during a standing pose similar to the observed deviations [4], [37], as well as offsets in the estimated kinematics due to imperfections in marker placement [36]. Still, irrespective of the differences with respect to the reference system, the system is able to reliably track kinematics across sessions, for example to assess clinically relevant functional activities [38]. To further support our speculations on the cause of the offsets observed for the hip flexion/extension and knee abduction/adduction, the N-pose assumption that was used for the above analysis was removed and a static pose directly obtained from the OpenSim

model has been applied instead at calibration phase, in order to carry out a more fair comparison between the two systems. In this case, as shown in Table II, the differences between MVN Analyze and OpenSim are smaller, specifically resulting in the mean RMS difference to become  $4.8 \pm 2.9$  instead of  $10.1 \pm 5.6$  for the hip flexion/extension and  $4.4 \pm 1.7$  instead of  $7.3 \pm 2.9$  for the knee abduction/adduction.

From Fig. 5, it is also easy to observe that knee and ankle angles are estimated in their three components in a similar way by both MVN Analyze and the OpenSim FDOF model. This is hinting to the fact that the OpenSim RDOF model, contrary to MVN Analyze and OpenSim FDOF, may be modeling these joint angles in a too simplistic way, leading to an inaccurate estimate of the actual joint movements.

To summarize, the observed differences are in line with



Fig. 8. Three example applications for the use of MVN Analyze.

observations from literature [4], [36], [39]. The angle differences in the sagittal plane, after applying the correction for the initial pose, are below 5 degrees for the three joints. The angle differences outside the sagittal plane are mostly slightly larger in Table I and II, but Fig. 5 reveals that the variance of the joint angles outside the sagittal plane of MVN Analyze and the OpenSim FDOF model, indicated by the semi-transparent areas, are in line with the observed differences and other studies [36]. On top of that, some of these angles for the knee and ankle are not estimated at all in the standard OpenSim RDOF model.

#### B. Running

The second dataset consisted of 10 healthy young athletes who were asked to run at three different speeds (10, 12, and 14 km/h for 3 minutes) on a treadmill. Data was captured again using *MVN Link* and processed using the *No Level* scenario in the *reprocess HD* mode of MVN Analyze. The objective of this dataset is to show that the joint angles are extracted in a consistent way for more challenging movements (running) even in magnetically challenging environments (treadmill).

The joint angles for the right leg of a representative subject are shown in Fig. 6. The figure shows the three joint angles during 3 minutes of running at 12 km/h, as well as the averaged joint angle by applying a moving average over 10 s for ease of interpretation. It can be clearly seen that the joint angles are consistently tracked during prolonged running in a magnetically challenging environment. Similar considerations hold for the other leg as well as all the other subjects. The consistency is also supported by Fig. 7, which shows a box and whisker plot for each averaged joint angle of the right leg for all 30 trials. The trials are ordered by the 3 different speeds and subjects are visually separated by the vertical lines. Although the positioning ( $y$  values) of each box may expectedly vary across subjects and speeds, it is important to notice that the size of each individual box is always small, indicating little dispersion of values of the averaged joint angles. Overall, the analysis indicates that the joint angles are consistently estimated for the complete dataset, which included a total of more than 90 minutes of running from 10 different subjects. Note that, if the angle calculations were affected by magnetic distortions, inconsistencies would show up in the form of a slow change of angle pattern over time and crosstalk between the joint angles in Fig. 6. Similarly, the moving average would be affected resulting in an increased size of the boxes and whiskers in Fig. 7.

#### V. CONCLUSION

In this whitepaper, the newly released Xsens MVN was presented and the performance of the MVN Analyze engine was compared against a reference, based on optical data in combination with two inverse kinematics models in OpenSim for healthy subjects who were walking at different speeds. In addition, the consistency of MVN Analyze was assessed by processing an extensive running dataset at three different speeds and analyzing the joint angles of the lower extremities. The comparison with OpenSim showed overall results in line with literature. The RMS differences for the angles in the sagittal plane were below 5 degrees. For the angles outside the sagittal plane, differences were slightly larger. It should be noted that the standard OpenSim RDOF constrains the angles at the knee and ankle and thus does not estimate these angles outside of the sagittal plane. Nevertheless, the OpenSim model without these constraints showed good correspondence for these angles with MVN Analyze, indicating the validity of the estimated angles. The analysis on the running data revealed that the joint angles for the hip, knee, and ankle were consistently estimated for the full dataset containing over 90 minutes of running data at a varying speed in a magnetically challenging environment.

The new engine enables reliable and consistent tracking of human body kinematics in any environment. Rich quantitative data can be obtained in the form of joint angles, segment positions, velocities, accelerations, and more, which allow other relevant quantities of interest to be derived. Fig. 8 shows some examples related to quality of exercise or performance for applications around sports, rehabilitation, and ergonomics.

#### VI. ACKNOWLEDGMENT

The authors would like to thank Jason Konrath PhD for his help in analyzing the motion capture data.

#### REFERENCES

- [1] G. Welch and E. Foxlin, "Motion Tracking: No Silver Bullet, but a Respectable Arsenal," *IEEE Comput. Graph. Appl.*, vol. 22, no. 6, pp. 24–38, 2002.
- [2] D. Roetenberg, *Inertial and Magnetic Sensing of Human Motion*. PhD Thesis, University of Twente, 2006.
- [3] W. H. K. de Vries, H. E. J. Veeger, C. T. M. Baten, and F. C. T. van der Helm, "Magnetic Distortion in Motion Labs, Implications for Validating Inertial Magnetic Sensors," *Gait & Posture*, vol. 29, no. 4, pp. 535–541, 2009.
- [4] X. Robert-Lachaine, H. Mecheri, L. C., and A. Plamondon, "Accuracy and Repeatability of Single-Pose Calibration of Inertial Measurement Units for Whole-Body Motion Analysis," *Gait & Posture*, no. 54, pp. 80–86, 2017.

- [5] E. B. Bachmann, *Inertial and Magnetic Tracking of Limb Segment Orientation for Inserting Humans into Synthetic Environments*. PhD Thesis, Naval Postgraduate School, 2000.
- [6] D. Roetenberg, H. J. Luinge, C. T. M. Baten, and P. H. Veltink, "Compensation of Magnetic Disturbances Improves Inertial and Magnetic Sensing of Human Body Segment Orientation," *IEEE Transactions on Neural Systems and Rehabilitation Engineering*, vol. 13, pp. 395–405, 2005.
- [7] X. Yun and E. R. Bachmann, "Design, Implementation, and Experimental Results of a Quaternion-Based Kalman Filter for Human Body Motion Tracking," *Robotics, IEEE Transactions on [see also Robotics and Automation, IEEE Transactions on]*, vol. 22, no. 6, pp. 1216–1227, 2006.
- [8] F. Dijkstra and P. J. Slycke, "Method and System for Enabling a Wireless Communication Between a Master Unit and a Sensor Unit," 2010. US Patent: US8947206 B2.
- [9] F. Dijkstra and P. J. Slycke, "A Method and a System for Enabling a Wireless Communication Between a Master Unit and a Sensor Unit," 2009. EU Patent: EP2320288 B1.
- [10] G. Bellusci, R. Zandbergen, and P. J. Slycke, "Reduced Processor Load for Wireless Communication Between Master Unit and Sensor Unit," 2014. US Patent: US9526028 B2.
- [11] G. Bellusci, R. Zandbergen, and P. J. Slycke, "Reduced Processor Load for Wireless Communication Between Master Unit and Sensor Unit," 2015. EU Patent: EP2958337 B1.
- [12] F. Dijkstra, H. J. Luinge, G. Bellusci, and P. J. Slycke, "Reduction of IMU/AP Link Requirements for SDI," 2012. US Patent: US8952785 B2.
- [13] H. J. Luinge, F. Dijkstra, and G. Bellusci, "Reduction of Link Requirements of an Inertial Measurement Unit (IMU/AP) for a Strapdown Inertial System (SDI)," 2013. EU Patent Application: EP2645061 A3.
- [14] H. J. Luinge, G. Bellusci, and F. Dijkstra, "Compression of IMU data for Transmission of AP," 2012. US Patent: US8981904 B2.
- [15] H. J. Luinge, F. Dijkstra, and G. Bellusci, "Compression of IMU data for Transmission of AP," 2013. EU Patent Application: EP2645110 A1.
- [16] H. J. Luinge, D. Roetenberg, and P. J. Slycke, "A System and a Method for Motion Tracking Using a Calibration Unit," 2007. EU Patent: EP1970005 B1.
- [17] H. J. Luinge, D. Roetenberg, and P. J. Slycke, "System and a Method for Motion Tracking Using a Calibration Unit," 2008. US Patent: US7725279 B2.
- [18] H. J. Luinge, D. Roetenberg, and P. J. Slycke, "Motion Tracking System," 2007. US Patent: US8165844 B2.
- [19] D. Roetenberg, P. J. Slycke, and P. H. Veltink, "Motion Tracking System," 2006. EU Patent: EP1959831 B1.
- [20] J. D. Hol and G. Bellusci, "Inertial Motion Capture Calibration," 2015. US Patent Application: US20160258779 A1.
- [21] J. D. Hol and G. Bellusci, "Inertial Motion Capture Calibration," 2016. EU Patent Application EP3064134 A1.
- [22] J. B. Kuipers, *Quaternions and Rotation Sequences*. Princeton University Press, 1999.
- [23] A. Vydyhanathan and G. Bellusci, "Xsens MTi White Paper: The Next Generation Xsens Motion Trackers for Industrial Applications." [https://www.xsens.com/download/pdf/documentation/mti/mti\\_white\\_paper.pdf](https://www.xsens.com/download/pdf/documentation/mti/mti_white_paper.pdf).
- [24] M. Paulich, H. M. Schepers, and G. Bellusci, "Xsens MTw White Paper: Miniature Wireless Inertial Motion Tracker for Highly Accurate 3D Kinematic Applications." <https://www.xsens.com/download/pdf/MTwWhitePaper.pdf>.
- [25] A. Cereatti, T. Bonci, M. Akbarshahi, K. Aminian, A. Barre, M. Begon, D. L. Benoit, C. Charbonnier, F. Dal Maso, S. Fantozzi, C. Lin, T. Lu, M. G. Pandy, R. Stagni, A. J. van den Bogert, and V. Camomilla, "Standardization Proposal of Soft Tissue Artefact Description for Data Sharing in Human Motion Measurements," *Journal of Biomechanics*, no. 62, pp. 5–13, 2017.
- [26] G. Bellusci, J. D. Hol, and P. J. Slycke, "Integration of Inertial Tracking and Position Aiding for Motion Capture," 2015. US Patent Application: US20170103541 A1.
- [27] J. D. Hol, H. J. Luinge, and P. J. Slycke, "Positioning System Calibration," 2011. EU Patent: EP2553487 B1.
- [28] J. D. Hol, H. J. Luinge, and P. J. Slycke, "Positioning System Calibration," 2010. US Patent: US8344948 B2.
- [29] J. D. Hol, F. Dijkstra, H. J. Luinge, and P. J. Slycke, "Tightly Coupled UWB/IMU Pose Estimation System and Method," 2009. US Patent: US8203487 B2.
- [30] P. H. Veltink, "Device and Method to Measure the Dynamic Interaction Between Bodies," 2008. US Patent: US8186217 B2.
- [31] G. Wu and P. R. Cavanagh, "ISB Recommendations for Standardization in the Reporting of Kinematic Data," *Journal of Biomechanics*, vol. 28, pp. 1257–1261, 1995.
- [32] G. Wu, S. Siegler, P. Allard, C. Kirtley, A. Leardini, D. Rosenbaum, M. Whittle, D. D'Lima, L. Cristofolini, H. Witte, O. Schmid, and I. Stokes, "ISB Recommendation on Definitions of Joint Coordinate System of Various Joints for the Reporting of Human Joint Motion - Part I: Ankle, Hip, and Spine," *Journal of Biomechanics*, vol. 35, no. 4, pp. 543–548, 2002.
- [33] G. Wu, F. C. T. van der Helm, H. E. J. Veeger, M. Makhsous, P. Van Roy, C. Anglin, J. Nagels, A. R. Karduna, K. McQuade, X. Wang, F. W. Werner, and V. Buchholz, "ISB Recommendation on Definitions of Joint Coordinate Systems of Various Joints for the Reporting of Human Joint Motion - Part II: Shoulder, Elbow, Wrist and Hand," *Journal of Biomechanics*, vol. 38, pp. 981–992, 2005.
- [34] E. S. Grood and W. J. Suntay, "A Joint Coordinate System for the Clinical Description of Three-Dimensional Motions: Application to the Knee," *Journal of Biomechanics*, vol. 105, no. 2, pp. 136–144, 1983.
- [35] S. L. Delp, F. C. Anderson, A. S. Arnold, P. Loan, A. Habib, C. T. John, E. Guendelman, and D. G. Thelen, "OpenSim: Open-Source Software to Create and Analyze Dynamic Simulations of Movement," *IEEE Transactions on Biomedical Engineering*, no. 54, pp. 1940–1950, 2007.
- [36] M. G. Benedetti, A. Merlo, and A. Leardini, "Inter-Laboratory Consistency of Gait Analysis Measurements," *Gait & Posture*, vol. 38, pp. 934–939, 2013.
- [37] R. Vialle, N. Levassor, L. Rillardon, A. Templier, W. Skalli, and P. Guigui, "Radiographic Analysis of the Sagittal Alignment and Balance of the Spine in Asymptomatic Subjects," *The Journal of Bone & Joint Surgery*, vol. 87, no. 2, pp. 260–267, 2005.
- [38] K. Al-Amri, M. Nicholas, K. Button, V. Sparkes, L. Sheeran, and J. L. Davies, "Inertial Measurement Units for Clinical Movement Analysis: Reliability and Concurrent Validity," *Sensors*, vol. 18, pp. 1–29, 2018.
- [39] J. L. McGinley, R. Baker, R. Wolfe, and M. E. Morris, "The Reliability of Three-Dimensional Kinematic Gait Measurements: A Systematic Review," *Gait & Posture*, vol. 29, pp. 360–369, 2009.